Experimental Systems

The past year has seen many new and exciting developments on the floor of the ALS. The protein crystallography wiggler beamline, driven by a 2-T multipole wiggler source, is now almost complete. The system is conventional in that it uses collimating and refocusing optics before and after a two crystal scanning monochromator. However, the very high power from the wiggler makes it necessary to intensively cool all the major optical elements, as well as slits and apertures. Even with only 1/3 of the ultimate aperture, the system will be one of the best in the world for crystallography. The first users of the beamline are scheduled to begin work in July 1997.

The scanning transmission x-ray microscope (STXM) on undulator Beamline 7.0 is now a mature instrument and is routinely taking data. This system uses zone plate focusing to produce a micro-focus, and, commensurate with the outer line width of the zone plate, the system is achieving around 1200-Å resolution. It has been used on a wide range of materials science problems, but work has especially concentrated on polymeric systems. The STXM works either in air or with one atmosphere of helium. To complement this instrument, an ultra-high vacuum system has been constructed and is now being commissioned. Again, it uses micro-zone plate focusing but in this case an electron energy analyzer is used for detecting photoelectrons (XPS). In addition to XPS, x-ray absorption spectroscopy (XAS) can be performed by detecting the total or partial yield of photoelectrons.

Bend magnet beamline 7.3.1 is now complete and in use. This beamline has two branches, one wide-aperture branch (7.3.1.1) for a photoelectron emission microscopy (PEEM), and a second branch (7.3.1.2) for micro-focused x-ray photoelectron spectroscopy (μ-XPS). The μ-XPS branch is finished and performing as expected. The system forms a monochromatic focus at an adjustable 20 by 40 μm pinhole, and this acts as an object for the following microscope. The focusing system is a pair of elliptically shaped grazing incidence mirrors, produced by controlled bending, which are within the ultra-high vacuum of the photoemission system. The microscope is designed to perform 1-μm-spatial-resolution scanning XPS on semiconductor wafers. It has many features specially designed for wafer samples, including in-situ high resolution optical microscopy, fast sample interchange, and interferometric encoding of sample position. One of the goals is to be able to introduce wafers into UHV, and go to previously referenced areas of interest to sub-micron accuracy. The development of this system is supported by Intel Corporation and Applied Materials.

Beamline 1.4 for infrared microscopy is nearing completion, the microscope is fully tested, and first beam is expected in April 1997. The system consists of two mirrors (plane and ellipsoidal) inside the shield wall to focus the radiation through a diamond isolation window; a system of collimating mirrors; and a commercial Nicolet interferometer and microscope. The wavelength range of 2–35 μm corresponds to the chemical fingerprinting range for organic species. Eventually, we will construct a second branchline to feed several different experiments including a system for reflection infrared studies of molecular adsorbates on clean single crystal surfaces.

The photoelectron emission microscopy beamline (7.3.1.1) is essentially complete and the PEEM system itself has an expected completion date of August. The PEEM endstation is derived from an earlier version produced by an ALS user group but differs in several key respects. It operates at high voltage (30 kV), has 2 projector stages, a stigmator and several deflectors to ensure that the beam passes through the center of the lenses, and fast sample transfer and sophisticated sample manipulation. A thorough theoretical study has shown that the system should be capable of 200-Å resolution and great attention is being paid to vibration isolation.

A second PEEM system is now under intense study and construction will start later this year. The 200-Å resolution limit, and the relative inefficiency of transmission (due to vignetting at the back focal plane aperture), are both consequences of the broad electron energy distribution produced by x-ray induced photoemission and the chromaticity of the electron lenses. It was recently shown by the group of Gertrude Rempfer (U. of Oregon Portland) that an electron mirror can be designed to have equal and opposite chromatic and spherical aberration coefficients to the combined electron optical column, and therefore opens up the possibility of very high spatial resolution with high throughput. The key components are the electron mirror and a magnetic prism to separate the incoming from the outgoing electron beams. This project is being jointly pursued with a group at Arizona State University. This system will need the very high flux density of the elliptical polarization undulator to reach its potential resolution of 2 nm. We expect completion of this project by fall 1998, commensurate with commissioning of the 4.0.3/4 microscopy beamline.

The first of the elliptical polarization undulator beamlines, 4.0.1/2, is now taking shape and a contract has been placed for construction of its high-power monochromator with Oxford Instruments. This beamline is designed for a wide energy range, 20–1600 eV, and will give very high resolving power for a range of studies on magnetic systems. Several of the optical elements are being fabricated, with the rest of the orders due for placement in spring 1997. The specification for the front end is also complete. ALS engineers are designing the complex mirror system located before the monochromator that will be used to focus radiation from either of the two elliptical polarization undulators into either of the two beamlines (4.0.1/2, 4.0.3/4). We expect operation of the first beamline in April

1998 and we have now started on the optical design of the second monochromator which will be optimized for high spatial resolution microscopy.

Reported byHoward Padmore

Adaptive-Mirror R&D

It is an axiom of the field of synchrotron radiation optics that the only beamline components that the *x-rays* ever see are the optical surfaces, many of which are mirrors. This emphasizes the true importance of forming optical surfaces in the best possible way and points first to the classical methods of grinding and polishing rigid glass mirrors. These techniques have been enormously successful in the wider field of optics and are still of value in some beamline applications. However, there are many cases where focusing mirrors must be made with tunable focal properties in which case one needs to make a circularly cylindrical mirror with a tunable radius. Another rationale arises when a mirror with a difficult shape is required. Often the mirror can be made flat and then be formed into an ellipse or other difficult shape by bending. This is not only less expensive than the zone-polishing techniques that would be needed to make a grazing-incidence ellipse, but it provides a superior figure and finish due the use of a full size lap in 100% contact with the mirror surface. Still other cases arise where the adaptive technology provides important correction capability against errors due to gravity, thermal distortion, or manufacturing tolerances.

In the ALS beamline construction program, the use of adaptive mirrors is increasing and the range of designs, materials, and applications is broadening due to an active R&D program by the Experimental Systems Group. At the time the ALS beamline program began, adaptive mirrors were already in use at several other synchrotron radiation laboratories and were also in wide use for optics that must see through the earth's atmosphere. However, the most recent generation of ALS beamlines always seemed to require new levels of optical quality (consequent upon the smallness of the ALS source), new materials properties, new shapes or sizes, or new levels of cost effectiveness. Such requirements (mostly derived directly from the needs of the scientific program) have lead to a number of advances in the art of adaptive mirrors which we describe below.

For adaptive mirrors, metals hold special advantages over ceramics because one can simply bolt them to a bending machine and bend them, to high curvature if needed, without fear of breaking. Ceramics on the other hand can be polished to a superior finish, have a proven dimensional stability, and an established ability to act as substrates for x-ray multilayers. To cover the widest range of possibilities, we need to use both so that we have to find metals that take a superpolish and have high dimensional stability and to establish safe methods of attaching glass and silicon mirrors to a bending machine. All these things have now been done as the following examples show (Table 2-2).

Table 2-2. Three elliptical mirrors made at the ALS.

	XPS* (BL 7.3.1.2)	PEEM (BL 7.3.1.1)	μDIFF* (BL 7.3.3.1)
Conjugates (m)	4, 0.1	20, 1.85	31, 0.1
Grazing angle (°)	1.6	2.5	0.33
Size (mm^3)	75×25×3	1250×100×15	40×10×3
Min radius (m)	4.5	48	32
Achieved slope error (μr)	2.2	5 (partial aperture)	0.6
Achieved finish (Å rms)	2.5	7	5
Projected spot size based on slope error (μm)	1	43	0.5
Material	precipitation-hardening stainless steel (17-4 PH)	fully-annealed, very-low-carbon steel (1006)	ULE™ (ultra-low expansion glass)
Polisher	Dallas Optical Systems	Rockwell (Albuquerque)	Rockwell (Albuquerque)
Attachments	nut and bolt	nut and bolt	glue
Special challenges	extreme curvature	avoid tension, extremely large size	figure accuracy

**Parameters of one of the pair are given as an example.*

All three examples have a number of features in common:

- *The shape is an elliptical cylinder*. The advantage of elliptical cylinders over circular ones lies in their aberration properties. For a given tolerance of aberration, the light-gathering power of the ellipse will always be greater, commonly by more than an order of magnitude for systems with a magnification far from unity. In a Kirkpatrick-Baez pair this advantage is squared.
- *The elliptical shape is generated by bending a mirror of uniform thickness but variable width.* This approach allows the most sensitive parameter (the thickness) to be accurately held uniform by precision grinding, lapping and polishing. The bent shape is determined by the width which is made to a calculated form by numerically-controlled machining.
- *The bending is carried out by weak leaf springs.* This type of bending delivers a prescribed force rather than a prescribed displacement which makes the system tolerant of manufacturing errors or changes in the mirror size (due to thermal expansion for example) so long as they are small compared to the driver motion needed to bend the mirror.

Three Example Mirrors

The mirror pair for the XPS project (Figure 2-13) was built for microfocusing with a goal of a 1 μm^2 focal spot at 1 keV and the maximum flux allowed by the beam phase space and the needed grazing angles of reflection. This implies elliptical mirrors to control aberrations and a high demagnification factor which in turn leads to a very high mirror curvature. To produce such extreme curvature and have a mirror thick enough to polish implies a high level of stress which suggests a metal substrate preferably without a plated layer. The development of mirrors made of precipitation-hardening stainless steel (17-4 PH) to meet all the needs of this application, including the achievement of a 2.5 Å rms finish on the bare steel, was achieved in a collaboration with small business and was one of the major successes of the program. The achievement of an elliptical mirror with this level of figure and finish was a first. The use of bare steel for such an enterprise was also a first which will have implications far beyond XPS. At time of writing, preliminary x-ray tests have shown a focal width of 3 μm.

The PEEM mirror offered quite different challenges. It was by far the largest mirror made at the ALS and was specified to as a condenser to illuminate a microscope sample with maximal flux over a field of 30 μm. As before it was necessary to make the mirror thick enough to polish and strong enough to take the bending stresses, and the solution was to use a common mild steel with very low carbon, for dimensional stability. A new type of crossed-leaf-spring bending machine was designed to avoid placing the mirror in tension and a plated layer of electroless nickel (to improve polishability) was applied to all the substrate surfaces. Such a layer could be safely used in this case since the surface stresses were about ten times lower than for the XPS mirror.

Figure 2-13. *The XPS experiment on Beamline 7.3.1.2 in which a Kirkpatrick-Baez pair of mirrors are used to form a finely focused spot of soft x rays. The two mirrors shown are made from simple stainless steel plates, suitably shaped so that when bending forces are applied, an elliptical-cylinder reflecting surface is formed. Such elliptical reflectors have much higher light gathering power than the corresponding circular ones.*

Unlike the other two mirrors, the microdiffraction mirror was for hard x-rays. This implied a much smaller grazing angle and a correspondingly weaker curvature to get a similar microfocusing geometry to the XPS system. This was accomplished by means of an edge-profiled ULE mirror glued to metal end pieces for connection to the bending springs. This mirror recently achieved the best slope error yet of 0.6 μr which is, in part, a tribute to a fairly to a significant research and development program in the use of glue for these types of optics. Apart from adequate strength, the adhesive material must have low outgassing and low shrinkage and must be applied so that such shrinkage as does occur is not in the longitudinal (curvature-producing) direction. At time of writing x-ray tests have also just begun on this system and first results show a 2.2 μm spot.

Reported by Malcolm Howells

The Micro-XPS Project

The micro x-ray photoelectron spectroscopy (μ-XPS) project is a joint development with Intel Corporation and Applied Materials. The object is to build an XPS system capable of 1 μm spatial resolution using a bend magnet source. The project grew out of a need identified in the Semiconductor Industry Association Roadmap for a technique capable of surface chemical mapping at high spatial resolution. Of existing techniques, infrared spectromicroscopy has excellent sensitivity and selectivity for organic species, but poor spatial resolution due to the diffraction limit for the long wavelengths used (typically 10-20 μm). On the other hand, scanning Auger microscopy (SAM) has excellent spatial resolution (0.1 μm), but the chemical information that can be obtained is extremely limited because the wide energy width of the Auger lines masks the subtle chemical shifts in binding energy that reveal chemical bonding.

In the semiconductor industry and many other areas where surface chemical information is important, there is a need for the combination of XPS with good spatial resolution. This need has led to the development of highly sophisticated laboratory systems for scanning XPS, and the current state-of-the-art achieves about 10 μm spatial resolution but has very long imaging times due to the limited brightness of the source. Our target was to design a system with a factor of 10 higher spatial resolution (1 μm), with short imaging times, and capable of taking full advantage of the tunability of synchrotron radiation. The selection of photon energy is important in two respects: first, it allows the cross section of the element of interest to be maximized; and second, it allows us to vary the kinetic energy of the photoemitted electrons and hence their escape depth. In this way we can alter the surface sensitivity and minimize radiation damage.

The ultimate goal will be to build a system with a resolution which is a small fraction of next generation microcircuit linewidths (0.25 μm). However, this would require the use of an undulator source and would be expensive. It is important at this stage to demonstrate the techniques in a user friendly system, rather than aim for the highest spatial resolution. The system we have designed addresses many of the concerns of the semiconductor community. For example, the system can accept 2 x 3 inch wafer sections, and, using a high resolution in-situ optical microscope to pick up fiducial points, a positioning accuracy of 1 μm can be achieved with laser interferometric encoding of the sample position. This is important because the patterned wafer samples will be first examined elsewhere using conventional techniques, the points of interest identified, and then the samples will be transferred to the ALS. Here they will pass through a fast entry load lock, through a prep chamber, and into the analysis chamber, while needing to retain the coordinate system of the sample to an accuracy matching our spatial resolution.

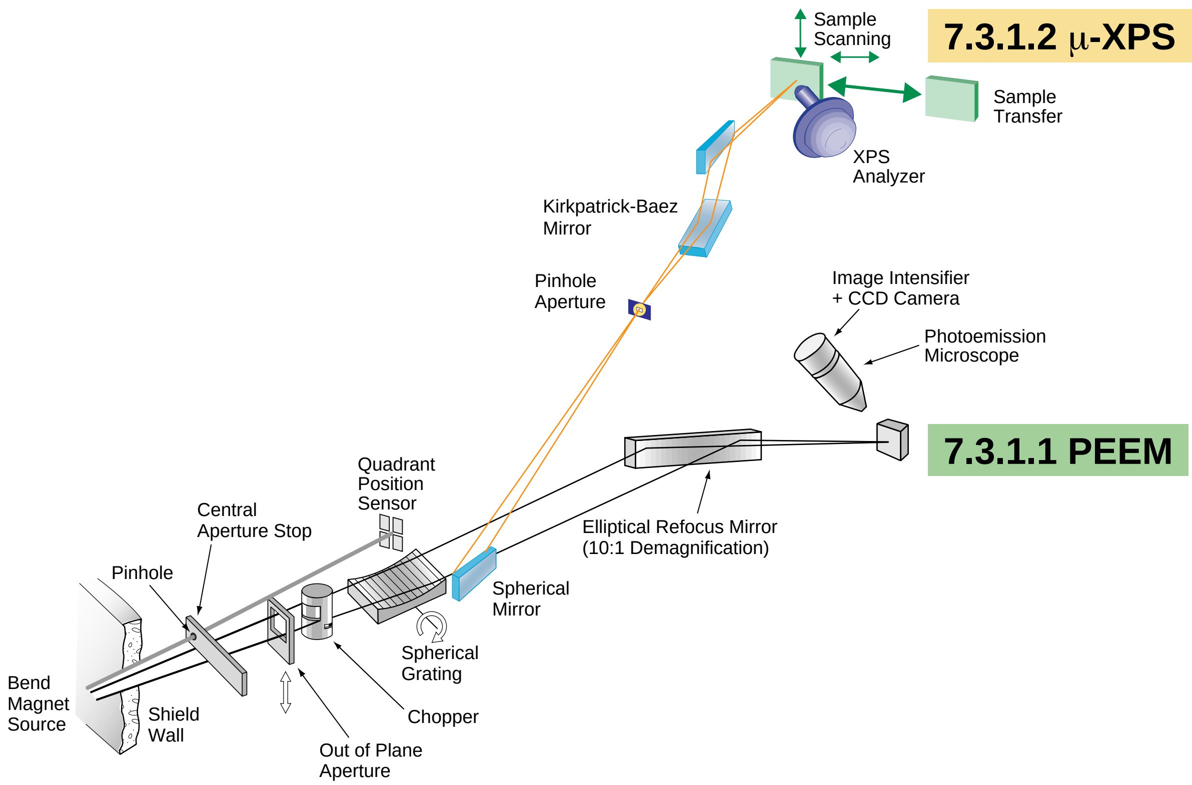

Figure 2-14. *Beamline 7.3.1 is a specialized beamline optimized for spectromicroscopy. It has two branches, one for magnetic imaging with a full-field imaging photoemission microscope (PEEM) and one for x-ray photoelectron spectroscopy (μ-XPS). A spherical mirror diverts part of the light from the main beam into the μ-XPS branch, so that both can be used simultaneously.*

The μ-XPS system uses a branchline off an existing monochromator, 7.3.1, in order to reduce the total system cost. This monochromator, together with a spherical horizontally deflecting branching mirror, delivers a monochromatic focus to an adjustable pinhole that then acts as the object for the μ-XPS imaging system. The micro-focusing is produced by orthogonal elliptical mirrors in a Kirkpatrick-Baez arrangement. These mirrors have to be near perfect to produce the micron-sized focus we desire, and are made by the controlled bending of flats (see "Research and Development in Adaptive Mirrors"). These focus at 40 and 20:1 in the horizontal and vertical directions respectively from the 40 x 20 μm object pinhole. The beam size at the mirrors is 1.25 x 2.5 mm, and, in a 100 and 200 mm image distance respectively, the beam is demagnified to 1 μm. In addition to the challenge of producing the elliptical mirrors, the whole optical system is in ultra-high vacuum and very close to the sample stage.

The system is now complete and undergoing initial commissioning. With almost no adjustment of the mirrors (there are 4 adjustments for each, only 1 of which has so far been used), the spatial resolution at full aperture is 2 x 7 μm. With further adjustment, we are confident of reaching our 1 μm target. In addition it should be noted that the diffraction limit of these mirrors at a photon energy of 1 keV is less than 0.1 μm, and so limited by the available photon flux, we can expect with improved optics and a smaller pinhole to achieve sub-micron resolution.

We anticipate a period of intense activity in which the ALS, Intel, and Applied Materials staff develop the system and apply it to microstructure materials problems. One of our near term goals will be to start work on an 8-in wafer stage, and, ultimately, if the return on investment is adequate, an undulator based system capable of 0.1 μm resolution.

Reported by Howard Padmore

Electrical and Mechanical Engineering

The unique capabilities and expertise of the ALS Mechanical and Engineering Groups are critical components in the ALS's mission to provide state-of-the-art instrumentation that will allow experimenters to conduct research at the forefront of their fields, and to develop new projects that will enhance the scientific capabilities of the facility both in the near term and in the more distant future. A few of the key areas of engineering R&D include insertion device design, beamline instrumentation, and accelerator diagnostics.

Insertion Device R&D

The 16-cm-period wiggler (W16) was completed and installed during the spring 1996 shutdown. This brought the total number of insertion devices installed in the ALS to five: four undulators and a wiggler. The wiggler will provide 5–15 keV photons for the Macromolecular Crystallography Facility located at Beamline 5.0. It features a variable gap, hybrid permanent magnet structure. Peak on-axis field is 2.17 T at the 14 mm minimum magnetic gap.

The second small-gap vacuum chamber was completed, this one destined for the U5.0 undulator serving Beamline 8.0. Installation of the chamber, scheduled for the May 1997 shutdown, will allow the undulator to reach 0.85 T peak effective field at the 14 mm minimum magnetic gap, providing photons just below 50 eV when the ALS operates at 1.5 GeV.

We started work on the 10-cm-period undulator (U10) that will serve the Atomic and Molecular Science Beamline to be moved from sector 9 to sector 10 in the later part of 1997. The photon energy range will be 12–1500 eV at 1.9 GeV. Though similar to first U10 undulator now in sector 9, this 43-period device uses the support structure, drive system, control system, and permanent magnet blocks available from the re-directed elliptical wiggler project as well as the vacuum chamber which will be removed from the undulator in sector 8 during the May 1997 shutdown. To reduce cost, the hybrid magnetic structure on this device utilizes iron instead of vanadium permendur for pole material. This is possible because the required peak field is only 0.8 T. The poles are designed to conveniently match the available vacuum chamber shape so additional machining on the chamber is not required.

In conjunction with the Experimental Systems and Accelerator Physics Groups, studies began on special insertion devices for such experimental areas as microdiffraction. Effort to date has been concentrated on determining performance from such devices as in vacuum, short period, small gap undulators; quasiperiodic undulators; superconducting undulators; high field wigglers; and single-pole bends. The goal of this study is to develop design parameters for future ALS insertion devices.

Reported by Egon Hoyer

Elliptical Polarization Undulator

Another key project of the ALS insertion device group in 1996 was the construction of the Elliptical Polarization Undulator and accompanying facility dedicated to magnetic microscopy and spectroscopy. We completed the final specifications and a detailed design for the first undulator, a 5-cm-period EPU5.0, and we began construction on the device and its related systems.

The 1.9-m-long EPU with 37.5 periods is designed to produce very bright photon beams with variable polarization in the energy range of 100–1500 eV. The EPU facility will eventually include two identical EPU5.0s and a third device with a longer period (approximately 8.0 cm, exact period length not yet determined) to access lower photon energies. The 1.9-m length is chosen to allow two insertion devices to be placed in tandem in a single straight. A third device is accommodated by use of a transverse stage on which one of the EPU5.0's will be mounted along with the longer period device. This arrangement will allow users to switch between the sources. A three magnet chicane system will separate the photon beams from the two insertion device stations by 2.53 mrad. The chicane system includes a magnet at the entrance and exit of the straight section and one between the two insertion devices. The straight section layout is shown in Figure 2-15.

Notable features of the EPU magnetic design include mechanical adjustability at each magnet to correct magnet errors that contribute to optical phase errors and electron beam trajectory perturbations, and a deflection- and displacement-free entrance and exit. The EPU5.0 is the first pure permanent magnet design for the ALS. It is also the first half-length device designed to accommodate two devices in a straight section.

The magnetic structure consists of four identical quadrants as shown in 2-16. Q1 and Q3 are fixed; Q2 and Q4 are allowed to translate parallel to the magnetic axis. The relative translation, called the quadrant phase, χ, of the magnetic quadrants, changes the ellipticity of an electron orbit passing through the device and thus changes the polarization of the emitted radiation. When $\chi = 0$, the magnetic structure is equivalent to a standard linear undulator, only B_y is produced on axis, and the radiation is linearly polarized in the horizontal plane. When $\chi = \lambda/2$, where λ is the undulator period, only B_x is produced on axis and radiation is linearly polarized in the vertical plane. When χ has any other value, both B_x

and B_y are produced on axis, and the radiation is elliptically polarized. When B_x=B_y, radiation is circularly polarized.

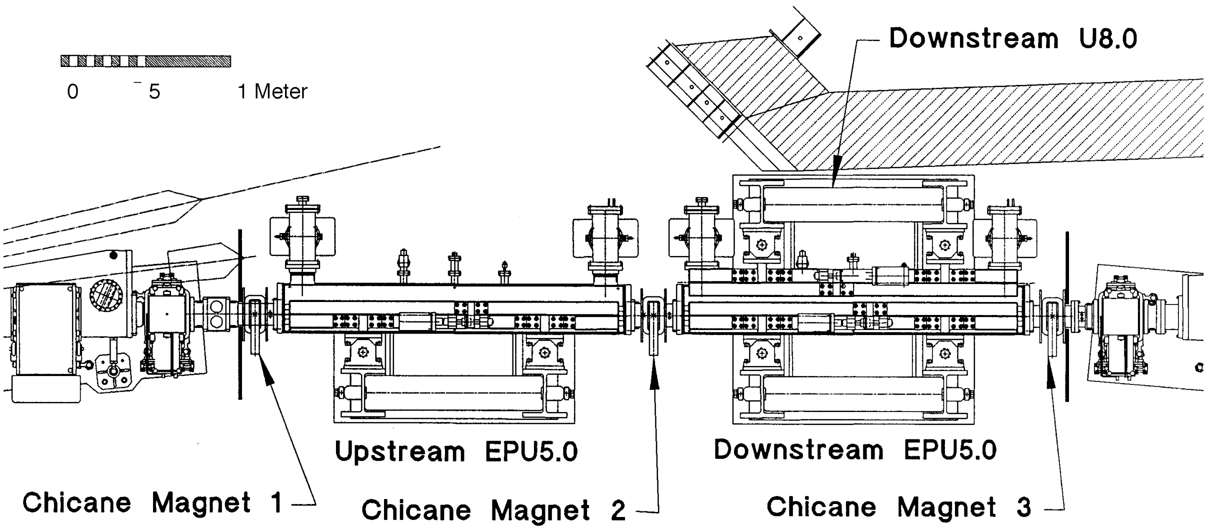

Figure 2-15. *EPU straight sector layout.*

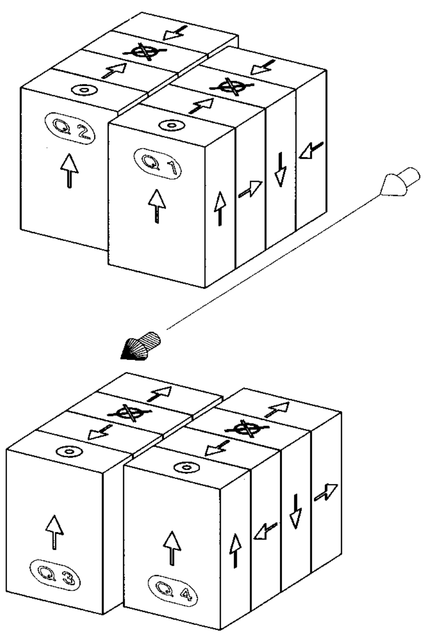

Figure 2-16. *Four quadrant schematic of the EPU.*

Several small magnetic models were assembled and used to test the magnetic design. A more elaborate 6.5 period prototype has also been completed. This has all of the magnetic features of the full device, including the ends. The model will be used to commission the new magnet measurement system, and to develop techniques for identifying and correcting magnetic errors. This will also give us our first test of whether or not we can achieve a gap-independent deflection- and displacement-free entrance and exit.

A new support structure and drive system was developed to accommodate as many as four shorter insertion devices in a single straight section: two source locations each with a possible arrangement of two side by side devices, either of which can be selected as the source. The drive system includes three drives: one to control the magnet gap, and two for translating the two moveable quadrants. The philosophy has been to make the design generic so that it may be utilized in future installations where two to four insertion devices per straight section are desired.

Reported by Steve Marks

Beamline Instrumentation

One piece of elegant engineering completed in only ten months was the branch of Beamline 7.3.1 to be used for micro-focused x-ray photoelectron spectroscopy (μ-XPS). Meeting a very tight manufacturing and commissioning goal was of key importance for the industrial partners, and excellence in design, engineering, and sustained support from the Berkeley Lab fabrication shops made it possible to meet this demanding schedule. The survey and alignment of the branchline was done with such accuracy that light reached the pinhole at the endstation in just under 2 hours of the initial attempt.

This Kirkpatrick-Baez arrangement of elliptically bent mirrors is unique. These mirrors are approximately 50 mm and 100 mm long with bending radii of 12 m and 6 m respectively. The slope errors of these mirrors after bending is less than 1 μrad. They are fabricated from precipitation hardened stainless steel and the stainless material was polished to 2.5 Å rms roughness—a first. The mirrors are aligned with respect to each other to 1 μm and form a spot size of 1 μm at the sample. 3D computer aided design was used to accurately determine the interaction of all the precision components and to aid in the measuring and fiducializing process.

The endstation system is located approximately 2 m above the floor and supported on a specially designed tetrahedron. The tetrahedron is a very rigid structure with a natural frequency of 60 Hz.

Reported by Ted Lauritzen

ALS High Resolution Beam Position Monitor

There are 118 electron beam position monitor (BPM) stations in the ALS storage ring. At each station there are four small electrodes called buttons that couple rf signals from the beam to processing electronics. Ninety-six of these monitors are in the 12 curved sections of the storage ring called sector-arcs. In these monitors, the buttons are connected to BPM electronics designed to provide high speed measurements of beam orbit. The remaining 22

BPM stations are in the straight sections, and the original purpose for these buttons was to act as pickups for a beam interlock system. If the electron beam in an insertion device is moved too far out of its normal orbit, it is possible for the powerful photon beam generated by the insertion device to melt areas of the aluminum vacuum chamber. When the interlock function of these BPMs is implemented, the beam will be aborted if a 2 mm orbit shift is detected in any straight section where an insertion device is operational. At present we rely on thermocouples attached to the beam pipe that sense heat generated by a miss-steered photon beam. The thermocouple system can be difficult to test and is designed to be a backup to the BPM interlock system.

High speed measurements are not required in order to implement the interlock feature, so it was decided to develop a high-resolution, narrow-band, multiplexed BPM instrument for the straight sections of the storage ring. Multiplexing four beam pickup signals into a single receiver at a high rate removes from the measurement many of the errors found in the non-multiplexed sector-arc BPM receivers. An additional feature of the new BPM is self normalization to beam intensity. This means the instrument delivers X and Y signals proportional to beam position regardless of the beam intensity (over normal ALS operating conditions). Because the BPM electronics are to be part of an equipment protection interlock, we chose not to rely on computer software—the electronics are completely analog. In the older BPMs, computers are needed to perform self calibration, correct gain and offset errors, perform normalization to beam intensity, and finally calculate beam position. It would be unwise to rely on such a BPM for an important equipment protection interlock.

High speed measurements are not required in order to implement the interlock feature, so it was decided to develop a high-resolution, narrow-band, multiplexed BPM instrument for the straight sections of the storage ring. Multiplexing four beam pickup signals into a single receiver at a high rate removes from the measurement many of the errors found in the non-multiplexed sector-arc BPM receivers. An additional feature of the new BPM is self normalization to beam intensity. This means the instrument delivers X and Y signals proportional to beam position regardless of the beam intensity (over normal ALS operating conditions). Because the BPM electronics are to be part of an equipment protection interlock, we chose not to rely on computer software—the electronics are completely analog. In the older BPMs, computers are needed to perform self calibration, correct gain and offset errors, perform normalization to beam intensity, and finally calculate beam position. It would be unwise to rely on such a BPM for an important equipment protection interlock.

The prototype insertion device beam position monitor (IDBPM) electronics were installed on a sector 4 straight section beam position sensor. The IDBPM revealed beam motion which had not been detected with the other BPMs. At that time the sector-arc BPM data were not being archived and no computer application was in use to display long-term beam motion. However, the IDBPM position data along with the temperature of the accelerator's cooling water and storage ring tunnel air were displayed on chart recorders over a period of many hours. From this data, it was quickly determined that the storage ring electron beam moved +/- 4 μm vertically with a period of about 12 minutes. Longer term vertical motion of about 20 μm occurred over several hours. Horizontal motion was larger, +/- 50 μm, with a period of about 2 hours. The chart recorder data showed perfect correlation between 12-minute vertical beam motion and magnet cooling water temperature fluctuations. Improvements were made to the water system temperature control, and the 12 minute beam position oscillations ceased.

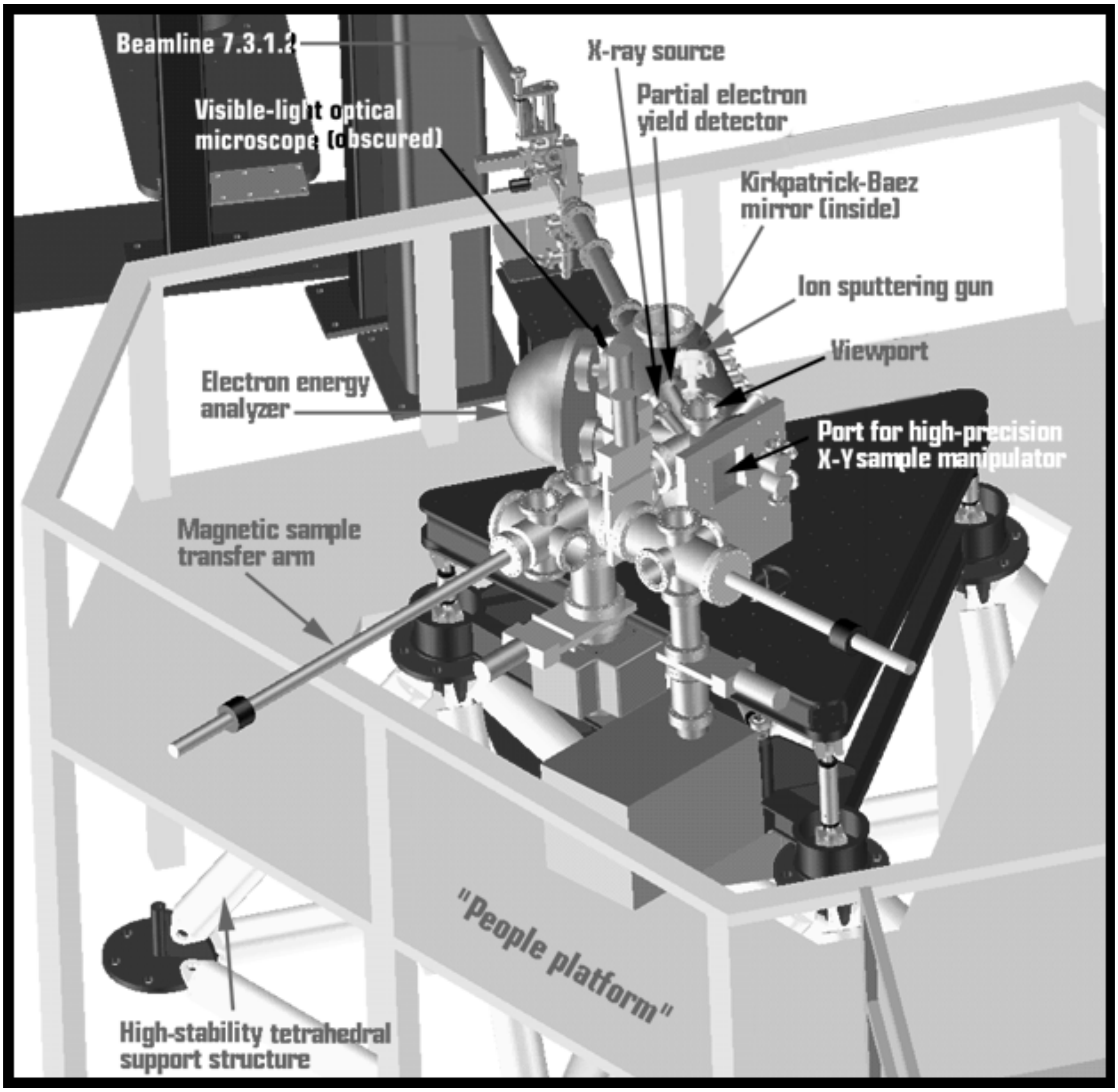

Figure 2-17. *A 3D CAD drawing of the microXPS system, showing beam entering from the left, the electron energy analyzer, sample manipulator, and sample prep systems. The microXPS endstation was created specifically for analyzing the microstructures and small-area interfaces in integrated circuits (ICs) and the silicon wafers from which ICs are made. It will be used for a variety of tasks in which the surface chemistry of microstructures needs to be determined. These include fundamental issues such as determining the chemical state of reacted surfaces and determining the composition of contaminant species.*

The IDBPM electronics were improved to reduce beam intensity dependent errors and another prototype instrument was installed. While BPM studies continued, the electronics design was offered to industry in hopes that a BPM useful to the accelerator community in general would be developed. The Bergoz company accepted the offer and improved the BPM electronics to the point where beam intensity dependence is almost nil and the input signal dynamic range is almost 10,000 to 1. For the ALS, this means we can obtain position readings over an intensity range of 0.4 A to less than 1 mA. Beam intensity dependence is typically less than 5 μm between 0.4 A and 1 mA when the beam is centered in the pickup electrodes. Resolution of less than 1 μm is easily achieved with signal averaging. As of February 1997, there were 6 Bergoz BPMs operating in the ALS storage ring, soon there will be over 20.

A beam stabilization task force was established at the ALS with the mission of determining the extent and causes of beam motion in the storage ring and to eliminate it if possible. The instruments used in this work are the IDBPMs, many temperature sensors, a number of electronic micrometers, and clinometers (devices capable of measuring very small angular displacement). The IDBPMs were connected to the ALS control system and their data displayed on a 12 hour chart in the control room. Also, the position data are archived along with all other accelerator parameters.

Our measurements have enabled us to reduce beam motion considerably, especially in the horizontal axis, in a relatively short time. The chief reason for this is good air temperature management. Our immediate goal is to stabilize vertical beam position over a filling period to about 2 μm (10% of the beam rms size in an insertion device). While air temperature control certainly helps, we believe we may have to employ a closed-orbit feedback system to achieve the ultimate stability. To implement closed orbit feedback, we require a number of stable position sensors around the storage ring. With 20 IDBPMs we should be able to reduce slow orbit shifts to some degree. For optimum performance, it may be necessary to have more position sensors. This would require additional Bergoz BPMs in place of (or in addition to) existing sector-arc BPMs.

Recent operational experience with the storage ring has shown that the "golden" beam orbit is not necessarily optimum for some insertion device beamline users. Because of their excellent stability, we have been using the IDBPMs to create a static local orbit bump around an insertion device to satisfy experimenters. If global closed-orbit feedback isn't implemented, it may be possible to apply local feedback around an insertion device to stabilize the photon beam. In this case the IDBPMs would be used as pickups for a local orbit bump feedback system.

The insertion device BPMs have been very useful in helping us diagnose undesired beam motion in the ALS storage ring. While they cannot provide the high-speed, single-turn beam position data we obtain from the sector-arc BPMs, they do provide unparalleled stability and resolution for low frequency position measurements. Once all the IDBPMs are functional and have been thoroughly tested, we will design the equipment protection interlock.

Reported by Jim Hinkson

Using Matlab for Accelerator Control

The ALS is a relatively small accelerator, yet the computer control system has the sizable task of continuously monitoring and controlling more than 7000 variables. Given this type of complexity, it is important to have an efficient method to acquire and control data.

The high-level software control of the ALS computer control system has been through a number of evolutions which pace the rapid developments in the computer world. While ALS computer control may lack the standard software development environment enforced at many modern accelerators, it gains in the amount of flexibility available to the application developer. ALS computer control is possible via BASIC, Visual Basic, C, C++ (Borland and Microsoft), FORTRAN, Pascal, Adelphi, TclTk, EPICS, Excel, Toolbook, and the list goes on. Since the variation of software is already large and convoluted, why not add one more—Matlab.

Matlab is a matrix manipulation language originally developed to be an efficient programming environment for using the LINPACK and EISPACK libraries developed in the heydays of FORTRAN. Hence, Matlab has a large number of built-in functions for numerical methods that have proven to be accurate, nearly bug free, and which properly warn the user if a calculation is close to a numerical instability. Matlab shares many similarities with other "high level" languages such as Mathematica, MATHCAD, and IDL. To gain the symbolic manipulation capabilities of languages like Mathematica, a version of Matlab can be purchased with the Maple kernel embedded. One big advantage of Matlab over FORTRAN, Pascal, or C is that matrix algebra is coded very much like one would write the equations on a piece of paper. However, it is very difficult to compare Matlab to a traditional compiled computer language. Matlab functions are compiled, but they run in an active workspace where each function call is interpreted at run time. Interpreted languages can be computationally slow, however, they allow one to create an interactive environment for doing mathematics on a computer. The fact that Matlab's built-in functions are compiled greatly mitigates the speed disadvantage of using an interpreted language.

What makes Matlab so appealing for accelerator physics studies is the combination of an active workspace for variables, numerous built-in functions, powerful graphics capability, and platform independence. At the ALS, Matlab is regularly used for global orbit correction, local steering of photon beams, developing insertion device dipole compensation tables, beam-based alignment of the quadrupoles, measuring response matrices, finding beta functions, and many accelerator physics studies.

The following example is the entire horizontal global orbit correction routine for the ALS using a singular valued decomposition (SVD) method where only the first 24 singular values of the matrix are used.

```
X = getx;      % Gets all 96 horizontal BPMs (96x1 vector)
[U, S, V] = svd(Sx);  % Computes the SVD of the response matrix, Sx(96x94)
DeltaAmps = - X / U(:,1:24); % Find the corrector changes via Gaussian elimination (94x1 vector
stepsp('HCM', DeltaAmps);    % Changes the current in all 94 horizontal corrector magnets
```

Once the ALS database access functions *getx* and *stepsp* (i.e. step the setpoint) have been written, this relatively involved global orbit correction method can be accomplished in four lines. Ease of use and simplicity allow one to quickly change and experiment with new ideas in a very short period of time. Given the value of machine time at the ALS, this is obviously a valuable tool.

Reported by Gregory J. Portmann

Ground Vibration and its Effect on Electron Beam Motion

Although the ALS building is a large structure with many thousands of tons of concrete in its foundation, the entire ALS floor is always being jostled around to some slight degree. The problem is not just the magnitude of the ground motion, but how these vibrations get amplified by the various structural bending modes of the ALS components. Here we report some preliminary results on how ground motion affects electron-beam motion.

If ground motion causes movement of the ALS photon beams, then many experiments at the ALS can be adversely affected. The mechanism for how ground vibration infiltrates into the photon beams is multifaceted. In the user areas, the entire beamline is subject to mechanical vibrations that simply shake the mirrors and endstation hardware. In the storage ring, vibrations move the magnets and vacuum chamber, which causes small field perturbations. These field changes cause electron beam movement, which in turn results in movement of the photon beams. The good news is that the ALS electron beam is inherently quite stable. Fluctuations in the electron beam in the 0.1 to 1000 Hz range are typically 3 to 8 μm rms, which is better than the specified requirement of one tenth of the beam size. This allows the ALS to operate without global or local orbit feedback, which is very unusual for a light source.

The level of ground vibration of the ALS floor is relatively small—typically less than a few tenths of a micron in the 0.1 to 400 Hz frequency range (the bandwidth of the accelerometers used to measure vibration). The problem arises from the mechanical amplification due to the natural bending modes of the magnet support structure and the magnification of magnet motion to electron beam motion due to the strong focusing quadrupole and sextupoles magnets in the storage ring. The magnification of beam motion from magnet motion is magnet family and location specific. Typical amplification factors range between 1 to 15. For instance, the peak electron beam motion for a change in position of a focusing quadrupole (QF family) magnet is a factor of 10 vertically and 6 horizontally greater than the magnet motion.

The aluminum vacuum vessel in the storage ring also influences beam motion. The first effect is beneficial: not all the magnetic field variations from a vibrating magnet will pass through the vacuum chamber. Due to the induced eddy currents in the aluminum, the magnet field as seen by the electron beam will be a low-pass filtered version of the actual perturbation. The exact bandwidths of these filters are magnet location specific and not well known but are likely to be a few Hertz. Unfortunately, the second effect is adverse: if the vacuum chamber is vibrating, the electron beam may pickup the high frequency motions since the eddy currents will oppose fast field changes inside the chamber.

Determining the sources for electron beam motion in the ALS storing ring is a difficult task. Vibration of the 72 quadrupole, 24 sextupole, and 36 bend magnets are likely sources, as well as field perturbations cause by the 216 power supplies in the storage ring (1 bend, 2 sextupole, 49 quadrupole, 94 horizontal corrector, and 70 vertical correctors). Measuring the beam motion is complicated by the fact that the BPMs are fixed in the vacuum chamber which is also vibrating. However, by measuring the electron beam motion, vibration of the magnets, and vibration of the vacuum vessel, the picture gains some clarity.

The upper plot in Figure 2-18 shows the power spectral density (PSD) function for the vibration of a quadruple focusing magnet (QFA 1 in sector 7), the vibration of the vacuum chamber in the location of the insertion device beam position monitor IDBPM(7,1), and the electron beam motion as measured by IDBPM(7,1). Vibration was measured using a seismic accelerometer from Wilcoxon Research (model 731A) connected to a spectrum analyzer (HP-3563A). Off-line analysis was done using Matlab. The bandwidth of the IDBPM is about 1 kHz. Unfortunately the noise floor of the IDBPM is not fully determined. The integral of the PSD function is the rms change in the time domain (Parseval's Theorem). Hence, using the power spectrum one can gain insight into what frequency bands are causing the greatest amount of beam motion. The lower plot in Figure 2-18 shows the cumulative integration of the power spectrum. The integration was done in reverse order, 50 Hz to 0.3 Hz, to illustrate the stability improvements if a feedback system was developed. For example, if one could eliminate all electron beam motion below 30 Hz, then the remaining motion would be 0.7 μm. However, this article is not accounting for motion above 50 Hz. Since electron beam motion in the 50 to 1000 Hz range is likely to be submicron, the signal-to-noise ratio of the IDBPM electronics becomes problematic.

The most obvious example of beam motion from vibration in Figure 2-18 is the 6.4 Hz bending mode of the storage ring girder. The first 4 structural modes of the girder, as reported in P.A. Manning and R.B. Burdick, "Dynamic Analysis of a Six Strut System," LLNL/SSC Presentation, June 19, 1992, are 6.4, 9.7, 12.7, 15.3 Hz. These 4 modes also show up clearly in the vibration data for the QFA magnet. Since the 6.4 Hz mode is not present in the vacuum chamber where the IDBPM is mounted, it is reasonable to assume that the electron beam is actually moving due to this structural mode. If one integrates the PSD from 5 to 8 Hz (shown in Figure 2-18, lower plot), the magnitude of this mode is approximately 0.6 μm. However, removing this mode would only reduce the total rms displacement from 3 to 2.9 μm ({EMBED Equation.2}). The 9.7 and 12.7 Hz modes also appear in the beam position spectrum. The 27 Hz peak in the IDBPM data makes a noticeable change in the rms motion, yet its source has not yet been determined.

Interpreting the downward slope in the lower plot of Figure 2-18 from 0.3 to 5 Hz can be done with the help of G.E. Fisher, "Ground Motion and its Effects in Accelerator Design," SLAC Pub. 3392, July 1985. Fisher has written an excellent survey paper on measuring ground vibration and the effects on accelerators. If the Wilcoxon accelerometers could resolve lower frequencies with a smaller noise floor, one would hopefully find a peak at 0.15 Hz caused by the ocean waves. Fisher reports that the ground vibration due to the ocean can be seen almost everywhere is the world—it is not just a coastal effect. The IDBPM data does not show this effect since the wavelength is long compared to the size of the ALS. The "bulge" in the data from 5 to 50 Hz is most likely caused by relatively local environmental sources.

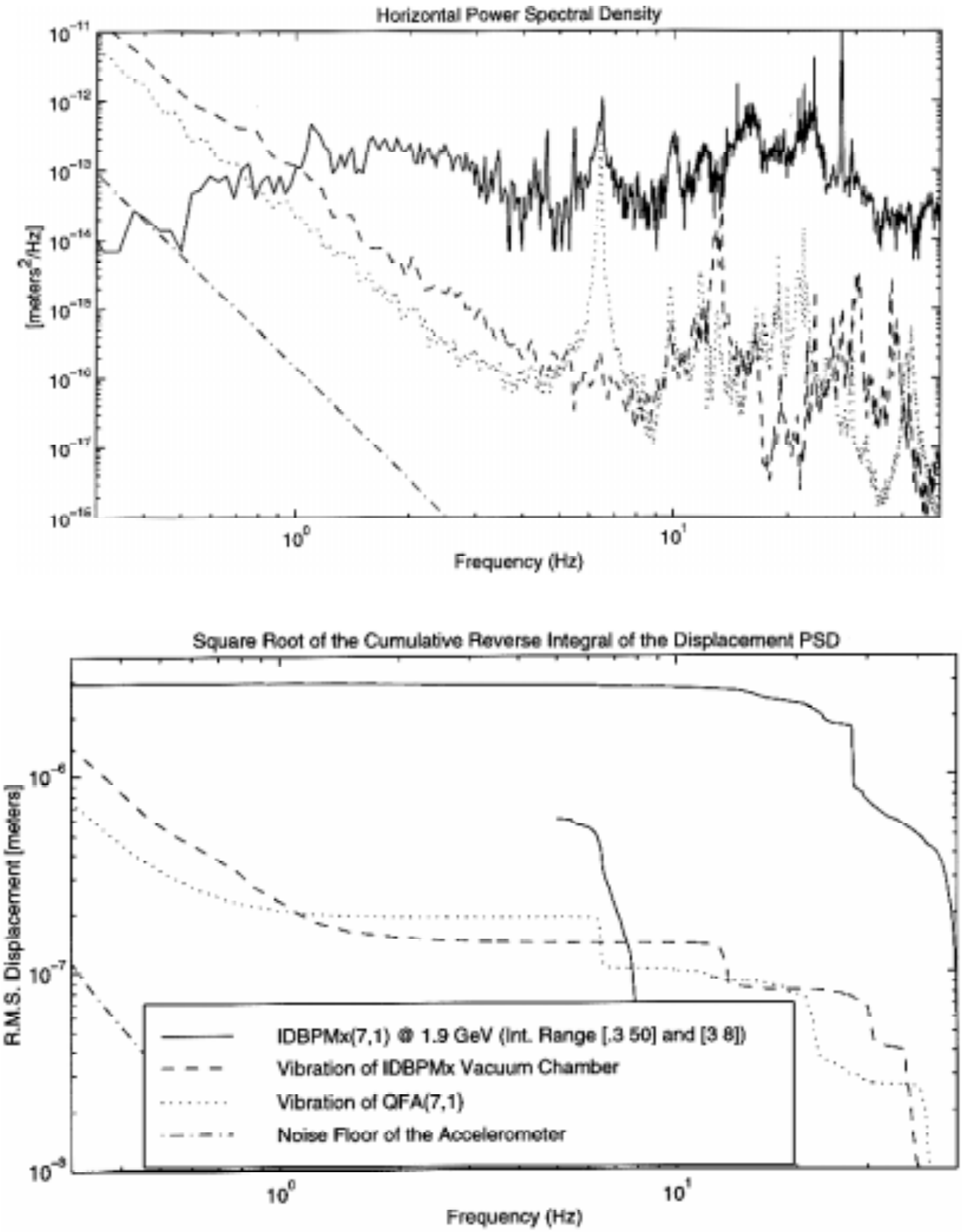

Figure 2-18. *The power spectral density (PSD) function for the vibration of a quadruple focusing magnet [QFA(7,1)], the vibration of the vacuum chamber in the location of the insertion device beam position monitor IDBPM(7,1), and the electron beam motion as measured by IDBPM(7,1).*

It is difficult to make a conclusive statement about the effects of vibration on electron beam motion from the limited amount of data presented in this paper. However, we feel it is reasonable to state that the magnitude of the motion caused by vibration is likely to be at the micron level. In order to form a more coherent picture as to the causes of “low” frequency beam motion at the ALS, one needs to combine vibration and power supply stability data with beam position data. Since the total electron beam motion in the 0.1 to 1000 Hz range is relatively small (a few microns), no serious attempt has been made to accurately determine the sources of the beam motion. If future experiments require electron beam stability below a few microns, then it will be necessary to either track down and eliminate the sources causing the motion or implement a feedback system to actively stabilize the electron and/or photon beams.

Reported by Gregory J. Portmann

Mechanical Design of a Pinger System for the ALS

As more beamlines are added to the ALS, tuning the storage ring for precise electron beam position and stability at all beamlines becomes increasingly difficult. To meet this challenge, ALS accelerator physicists are working to improve their understanding of the complex electron beam dynamics of the storage ring. The new "pinger system," currently in the design and fabrication stage, will be an important tool in this effort.

Specifications

The pinger system will provide a pair of very fast dipole magnets to intentionally perturb the orbit of a single electron bunch in a single pass. The effects of this controlled transverse "kick" will be monitored by an existing system of beam position monitors (BPMs) for validation and improvement of beam dynamics models. In order to accomplish this, the pinger system must deliver calibrated vertical and/or horizontal dipole fields of up to 315 Gauss in a pulse which lasts no longer than 650 ns. This will require single turn dipole magnets, discharging 10 kV to ground. A special ceramic beam tube section is needed so that induced eddy currents will not retard the penetration of the magnet field.

Engineering

As is often the case, the initial intention for this project was to closely duplicate an existing design. The beam kickers in the ALS injection straight perform a similar function, and we hoped to save on engineering costs. However, as is also often the case, a closer study of the injection straight revealed many reasons not to do this. The following is a brief summary of the design evolution of the pinger system (an early concept sketch is shown in Figure 2-19). As you will see, considerable effort has gone into creating a cost effective, reliable design, with many well-motivated departures from the original concept.

Our reference design, the ALS injection straight, has a rectangular vacuum aperture of 83 x 38 mm^2. Its ceramic vacuum tube was expensive, difficult to manufacture, difficult to align, and the unbalanced vacuum forces are high. For the pinger, an 88-mm ID round ceramic beam tube was chosen to be much stronger and easier to fabricate, and its "square" aperture allows the horizontal and vertical kick magnets to be essentially identical. A further advantage emerged: in the round geometry, beam image currents can be handled by a uniform resistive coating on the tube ID, with no need for the difficult patterned resistive coating used with the rectangular aperture. The optimum coating resistance is a trade-off between minimizing the eddy-current-induced field penetration delay, and living with the steady state $P= I^2R$ heating of the ceramic tube caused by beam image currents of up to 400 mA. An experimental mock-up indicates that a 2.0-ohm-per-square coating of titanium will allow acceptable field penetration times with a maximum steady state image current heat load of about 100 watts, which will be cooled with an air flow system.

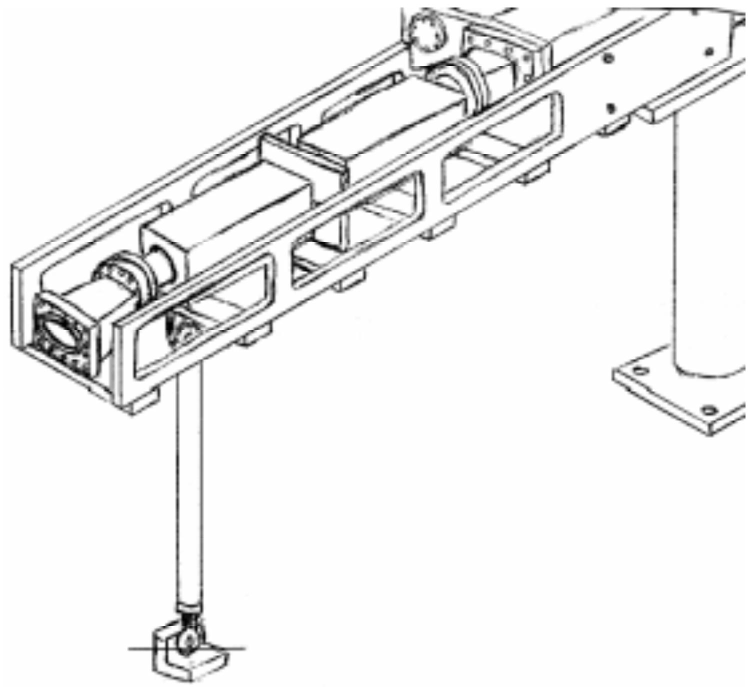

Figure 2-19. *An early concept sketch for the ALS pinger system.*

The original electrical joint design used to connect the injection straight resistive coating to the conventional metal beam tube has caused some concern at the ALS. Beam current induced heating at or very near these joints has necessitated forced air cooling. Although the cause of this problem has not been resolved, a leading theory is that small cavities in the electrical joint design may be coupling with rf energy, resulting in local heating. In the pinger design, only a single, round fingerstock joint is used, with a minimum cavity.

The various risks and expense of the ceramic tube end electrical and vacuum connections motivated a further simplification: a single long ceramic tube threaded through both the horizontal and the vertical kick magnets. A 54-in (1.37 m) tube length is required, with only two end connections, rather than the four which would have been needed with separate tubes for each magnet.

Support and alignment of the ceramic tubes in the injection straight had been a problem, due to variations in ceramic wall thickness. For the pinger, we will avoid this by not doing it.

We plan to rely only on the engagement of the electrical contact sleeve in the neighboring transition piece to flexibly support the 25-lb (11.34 kg) weight of the ceramic tube.

Axial vacuum loads were considerable in the injection straight design because of the difference in cross section between the bellows and the ceramic tube aperture. (The collapsing load of the bellows exerts a sizable tension load on the ceramic tube.) Since the pinger ceramic tube is round, it is possible to use a bellows of only slightly larger area than the tube itself. The calculated vacuum load tension in the pinger ceramic tube is much reduced, only 102 lb (46.27 kg). This load is taken in tension by the Kovar fittings brazed to the ends of the ceramic beam tube. The maximum stress in the critical braze joint was further reduced by making the O.D. of the ceramic backing ring 1.8 mm larger than the ceramic tube. A finite element analysis shows that this small change will reduce the maximum stress in the braze joint by a factor of six. These increased safety margins all work to improve the vacuum integrity of the ALS storage ring.

The pinger system will be installed in ALS straight section 2. The one-piece ceramic tube (Figure 2-20) allows the pinger to be short enough to occupy only the upstream half of the straight section, reserving the downstream half for future diagostic instruments, or possibly even an insertion device. In this location, photon masking had to be carefully considered; that is, the synchrotron radiation from the upstream bend magnet had to be absorbed by a water cooled photon stop incorporated in the upsteam transition piece. In the course of studying these layouts, a further simplification emerged: there is no need for the electron beam to be perfectly centered in the ceramic beam tube. By introducing an intentional offset of 10 mm, we were able to reduce the tube inner diameter from 88 mm to only 74 mm. This resulted in a reduced magnet aperture and a reduced pulsed power requirement.

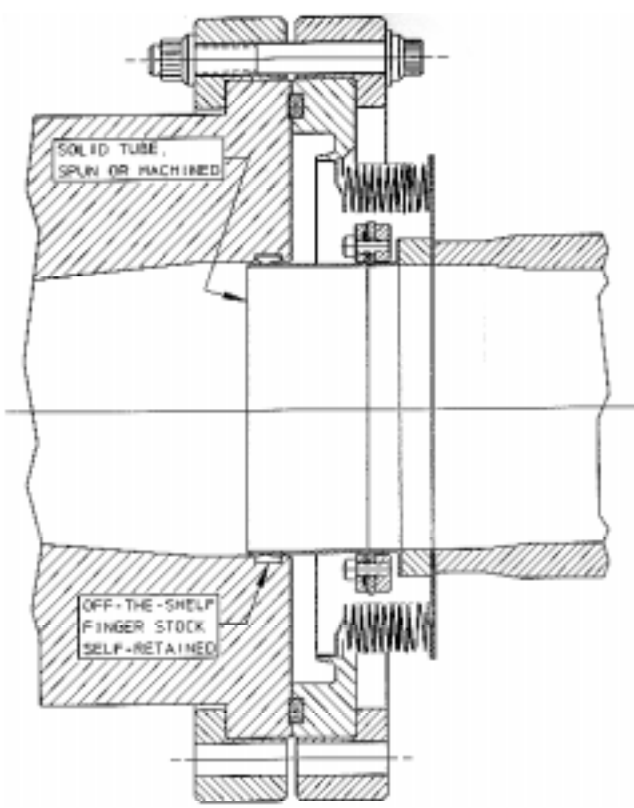

***Figure 2-20**. Ceramic beam tube design.*

With a robust, conservative design in hand, we confronted the realities of component fabrication. The ceramic tube with its brazed Kovar metal end fittings turned out to be an exceedingly involved fabrication. Over 20 different ceramic, metalization, and brazing vendors were contacted, revealing a wide variety of capabilities and limitations. Ultimately, the 1.35-m-long 99.5% alumina tubes were pressed, fired, and metalized in 0.68-m-long halves by WesGo, Inc. (Belmont, CA), and these were subsequently brazed together and to their Kovar metal end fittings by Alpha Braze (Fremont, CA).

Other design involvements include the "transition pieces" which are EDM'd (Electric Discharge Machined) from solid metal blocks to provide a smooth vacuum chamber transition from the elliptical section of the storage ring to the round ceramic tube, and a carefully thought out support system designed to protect the ceramic beam tube from mechanical stress. We are working hard to bring all the vacuum related components together in time for installation in the May 1997 shutdown of the ALS, and hope to deliver a working pinger system in summer 1997. Like many accelerator upgrade projects, an idea that initially sounded fairly straightforward has spawned a rich mix of engineering complications and challenges.

Reported by William Thur